Nonlinear wave interactions in supersonic windgenerated waves

Spyridon G. Lekoudis, Ali H. Nayfeh, and William S. Saric

Citation: Physics of Fluids (1958-1988) **25**, 1524 (1982); doi: 10.1063/1.863939
View online: http://dx.doi.org/10.1063/1.863939
View Table of Contents: http://scitation.aip.org/content/aip/journal/pof1/25/9?ver=pdfcov
Published by the AIP Publishing

Nonlinear wave interactions in supersonic wind-generated waves

Spyridon G. Lekoudis
School of Aerospace Engineering, Georgia Institute of Technology, Atlanta, Georgia 30332

Ali. H. Nayfeh and William S. Saric
Department of Engineering Science and Mechanics, Virginia Polytechnic Institute and State University, Blacksburg, Virginia 24061

(Received 19 March 1982; accepted 7 June 1982)

A nonlinear analysis is presented for the case of second-harmonic resonant interactions on the interface of a liquid film and a supersonic gas stream. The analysis takes into account the effects of the gas viscosity and mean profiles. Moreover, the extent of the gas disturbance layer is not restricted to the region in which the mean profiles are linear. Self-sustained oscillations are calculated for low and intermediate liquid Reynolds numbers. The present solution is compared with available experimental data. The predicted and observed wave amplitudes, wavenumbers, and frequencies are in good agreement for intermediate liquid Reynolds numbers. The calculated amplitudes overpredict the observed values by about a factor of three for low liquid Reynolds numbers.

I. INTRODUCTION

Information concerning the behavior of liquid films interacting with high-speed air streams has application to a number of different technological areas. Transpiration cooling of high-speed vehicles,[1,2] steam-turbine blade erosion,[3,5] magnetohydrodynamic power generators,[6] and leading-edge cleansing devices for airfoils with laminar flow control are a few areas that have received recent attention. Essential to studies of these different flow environments is the understanding of the stability characteristics of the liquid film. If the liquid is unstable, small drops will be entrained into the gas stream. In this case, the evaporative cooling protection is lost for transpiration systems,[7] but the erosion of steam-turbine blades is minimized.[5] If the liquid is stable, finite-amplitude waves appear on its surface, and information concerning the wave amplitude and the wavelength is important for the development of modified heat and mass transfer models.

Experiments have shown that under certain liquid conditions, the liquid film is stable when the gas flow is supersonic,[2,5] whereas the film may be either stable or unstable if the gas flow is subsonic.[5,7] When the surface of the film is disturbed, a number of stabilizing and destabilizing mechanisms come into play. A survey of these mechanisms and their application to the liquid film problem is given in Refs. 1, 5, and 6.

Linear stability theories predict that liquid films adjacent to supersonic streams are much more unstable than liquid films adjacent to subsonic streams, in disagreement with the experimental observations of Saric *et al.*[2] and Wurz.[5] However, the experimental observations can be explained qualitatively by using nonlinear theories.

Nayfeh and Saric[8] analyzed the nonlinear stability of a quiescent viscous liquid film parallel to an inviscid compressible gas for small liquid Reynolds numbers within the long-wave approximation. In the subsonic case, they found that unstable linear disturbances continue to be unstable in the nonlinear case; thus conditions exist for liquid entrainment by the gas, in qualitative agreement with the experimental observations. In the supersonic case, they found that stable linear disturbances dampen faster while unstable linear disturbances do not grow indefinitely but become steady periodic waves. Thus, conditions for entrainment do not exist in this case, in qualitative agreement with the experimental observations. In a later study, Nayfeh and Saric[9] removed the initial quiescent liquid assumption of their previous study by taking the liquid velocity profile into account.

Bordner and Nayfeh[10] refined the previous nonlinear stability models by relaxing the restriction on the magnitude of the liquid Reynolds number and by including the effects of the gas viscosity and velocity profile in calculating the pressure and shear perturbations exerted by the gas on the liquid/gas interface. Saric *et al.*[2] used the same model for the case of a turbulent gas boundary layer and showed that, in spite of all the improvements, the quantitative agreement with the available experimental data is still poor. The present study removes the assumption made by Bordner and Nayfeh[10] that the disturbance lies in the region in which the mean profiles are linear. Moreover, the linear dispersion relation (generated numerically) shows that resonance conditions exist in the lower range of wave numbers which include the experimentally observed ones. Based on this observation, a model is developed that accounts for second-harmonic resonant interactions, and the results are compared with available experimental data.

II. PROBLEM FORMULATION

Since the experimental results show that the liquid surface velocities and the wave speeds are very small compared with the gas freestream velocity, the liquid surface can be assumed to be stationary in calculating the pressure and shear perturbations exerted by the gas on the gas/liquid interface. Moreover, since the gas Reynolds number based on the observed wavelengths is large, the mean flow can be assumed to be parallel.

 0031-9171/82/091524-08$01.90

A. Equations for the liquid phase

Since the experimental results show that there is a range of conditions under which stable two-dimensional waves exist, in this paper we are concerned with these two-dimensional waves. A schematic of the flow is depicted in Fig. 1. The liquid is assumed to have a uniform density $\tilde{\rho}$ and viscosity $\tilde{\mu}$.

We introduce dimensionless variables as follows: The streamwise direction $\tilde{x}$ is made dimensionless by using the wave number $\tilde{\alpha}$ of an assumed sinusoidal disturbance, while the normal direction $\tilde{y}$ and liquid depth $\tilde{h}$ are made dimensionless by using the mean depth $\tilde{h}_0$. Flow quantities are made dimensionless by using interface conditions denoted by the subscript l. In addition, each of the flow velocities and pressure is resolved into a basic state and a disturbance component. Thus, we let

$$t=\tilde{\alpha}\tilde{u}_l t\,,\quad x=\tilde{\alpha}\tilde{x}\,,\quad y=\tilde{y}/\tilde{h}\,,$$
$$h=\tilde{h}/\tilde{h}_0\,,\quad u_0+u=\tilde{u}/\tilde{u}_l\,,$$
$$v=\tilde{v}/\alpha\tilde{u}_l\,,\quad p_0+p=\tilde{p}/\tilde{\rho}\tilde{u}_l^2\,,$$

where

$$\alpha=\tilde{\alpha}\tilde{h}_0\,,\quad u_0=\tilde{u}_0/\tilde{u}_l\,,\quad p_0=\tilde{p}_0/\tilde{\rho}\tilde{u}_l^2\,.$$

For the basic state, we have

$$u_0=y\,,\quad p_0=\tilde{p}_{0_s}/\tilde{\rho}\tilde{u}_l^2+G(y-1)\,, \tag{1}$$

where $G=\tilde{g}\tilde{h}_0/\tilde{u}_l^2$ is the inverse of the Froude number.

We also introduce a dimensionless stream function $\psi(x,y,t)$ defined by $u=\psi_y$, $v=-\psi_x$. The governing equations for the disturbance stream function, with a linear basic-state velocity profile, give

$$\psi_{yyyy}=\alpha R\left[\psi_{yyt}+(y+\psi_y)\psi_{xyy}-\psi_x\psi_{yyy}\right]-2\alpha^2\psi_{xxyy}+\alpha^3R\left[\psi_{xxt}+(y+\psi_y)\psi_{xxx}-\psi_x\psi_{xxy}\right]-\alpha^4\psi_{xxxx}\,, \tag{2}$$

where $R=\tilde{h}_0\tilde{u}_l\tilde{\rho}/\tilde{\mu}$ is the liquid Reynolds number. The no-slip and no-penetration boundary conditions at the solid surface give

$$\psi=0\quad\text{and}\quad\psi_y=0\quad\text{at}\quad y=0\,. \tag{3}$$

The kinematic boundary condition at the interface is

$$h_t+(h+\psi_y)h_x+\psi_x=0\quad\text{at}\quad y=h\,. \tag{4}$$

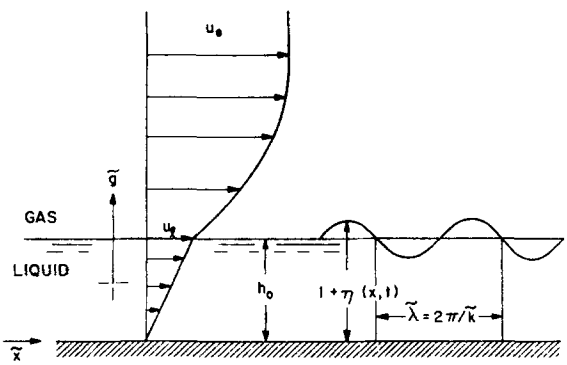

FIG. 1. Flow configuration. Basic state and disturbance.

The balance of normal and tangential stresses at the interface yields

$$\frac{\Lambda}{\alpha R}=G(h-1)+\frac{\alpha^2Wh_{xx}}{1+\alpha^2h_x^2}+\frac{2\alpha}{R}\psi_{xy}\frac{1-\alpha^2h_x^2}{1+\alpha^2h_x^2}+\frac{2\alpha}{R}\times(\psi_{yy}-\alpha^2\psi_{xx})\frac{h_x}{1+\alpha^2h_x^2}\quad\text{at}\quad y=h\,, \tag{5}$$

$$\chi=(\psi_{yy}-\alpha^2\psi_{xx})\frac{1-\alpha^2h_x^2}{1+\alpha^2h_x^2}-4\alpha^2\psi_{xy}\frac{h_x}{1+\alpha^2h_x^2}\quad\text{at}\quad y=h\,, \tag{6}$$

where

$$W=\frac{\tilde{T}_s}{\tilde{\rho}\tilde{h}_0\tilde{u}_l^2}\,,$$

$$\Lambda=\frac{\alpha R}{\tilde{\rho}\tilde{u}_l^2}\left(-\tilde{\sigma}(h)-\tilde{p}_{0g}-\frac{2\tilde{\tau}_0\tilde{h}_{\tilde{x}}}{1+\tilde{h}_{\tilde{x}}^2}\right), \tag{7}$$

$$\chi=\frac{R}{\tilde{\rho}\tilde{u}_l^2}\left(\tilde{\tau}(h)-\tilde{\tau}_0\frac{1-\tilde{h}_{\tilde{x}}^2}{1+\tilde{h}_{\tilde{x}}^2}\right), \tag{8}$$

with $\tilde{T}_s$ being the surface tension and W being the inverse of the Weber number. The pressure and shear perturbation parameters Λ and χ are obtained from the solution of the gas-phase problem.

B. Equations for the gas phase

All lengths in the gas problem are made dimensionless by using the wavenumber $\tilde{\alpha}$ of an assumed sinusoidal surface disturbance. All flow quantities are made dimensionless by using the freestream conditions denoted by the subscript ∞. Thus, we let

$$x=\tilde{\alpha}\tilde{x}\,,\quad Y=\tilde{\alpha}(\tilde{y}-\tilde{h})\,,\quad h=\tilde{h}/\tilde{h}_0\,,$$
$$u=\tilde{u}/\tilde{u}_\infty\,,\quad v=\tilde{v}/\tilde{u}_\infty\,,\quad \rho=\tilde{\rho}/\tilde{\rho}_\infty\,,$$
$$p=\tilde{p}/\tilde{p}_\infty\tilde{u}_\infty^2\,,\quad T=\tilde{T}/\tilde{T}_\infty\,,\quad \mu=\tilde{\mu}/\tilde{\mu}_\infty\,.$$

In terms of these dimensionless quantities, the equations describing the gas motion are

$$(\rho u)_x+(\rho v)_Y=0\,, \tag{9a}$$

$$\rho uu_x+\rho vu_Y+p_x=\frac{1}{R_G}\left\{\left[\mu\left(\tfrac{4}{3}u_x-\tfrac{2}{3}v_Y\right)\right]_x+\left[\mu(u_Y+v_x)\right]_Y\right\}, \tag{9b}$$

$$\rho uv_x+\rho vv_Y+p_Y=\frac{1}{R_G}\left\{\left[\mu(u_Y+v_x)\right]_x+\left[\mu\left(\tfrac{4}{3}v_Y-\tfrac{2}{3}u_x\right)\right]_Y\right\}, \tag{9c}$$

$$\rho uT_x+\rho vT_Y=(\gamma-1)M_\infty^2\left(up_x+vp_Y+\frac{1}{R_G}\Phi\right)+\frac{1}{PrR_G}\left[(\mu T_x)_x+(\mu T_Y)_Y\right], \tag{9d}$$

$$\gamma M_\infty^2\,p=\rho T\,, \tag{9e}$$

where γ is the gas specific heat ratio,

$$\Phi=\mu\left[2(u_x^2+v_Y^2)+(u_Y+v_x)^2-\tfrac{2}{3}(u_x+v_Y)^2\right], \tag{9f}$$

$$R_G=\frac{\tilde{\rho}_\infty\tilde{u}_\infty}{\tilde{\alpha}\tilde{\mu}_\infty}\,,\quad Pr=\frac{\tilde{C}_p\tilde{\mu}_\infty}{\tilde{\kappa}}\,,\quad M=\frac{\tilde{u}_\infty^2}{(\gamma-1)\tilde{C}_p\tilde{T}_\infty}\,. \tag{9g}$$

The dependence of viscosity on the temperature is assumed to be given by Sutherland's law

$$\mu = T^{3/2}(T+b)^{-1}, \tag{10}$$

where b is a dimensionless constant. At the interface, the condition that the velocity components vanish yields

$$u = v = 0 \quad \text{at} \quad Y = \alpha(h-1). \tag{11a}$$

For an adiabatic flow,

$$\frac{\partial T}{\partial Y} = 0 \quad \text{at} \quad Y = \alpha(h-1). \tag{11b}$$

The final boundary condition is the upstream vanishing of disturbances.

The basic state is assumed to be a laminar boundary-layer flow. The solution for this basic state is obtained numerically by solving the boundary-layer equations. The compressible boundary layer equations for two-dimensional laminar flow of the gas can be written in the form[11]

$$\frac{d}{dy}\left(c_1 \frac{dU_0}{dy}\right) + \left(c_2 \int_0^Y \frac{U_0}{T_0}\, dy\right)\frac{dU_0}{dy} = 0, \tag{12}$$

where the coefficients c_1 and c_2 are functions of the variable viscosity inside the shear layer, T_0 is the mean temperature, related to the mean velocity with Crocco's relation, and U_0 is the mean velocity in the streamwise direction. A standard tridiagonal inversion subroutine with iterative updating of the dependent variables is used to solve this equation. Detailed conditions of the gas flow are given in Ref. 2. No results are presented in this paper for the case of turbulent gas flow.

III. LINEAR STABILITY ANALYSIS

Next we analyze the linear stability of the liquid film. We shall assume infinitesimal disturbance at the liquid interface in the form of a traveling wave; i.e.,

$$h = 1 + \eta_1, \quad \eta_1 = A\exp[i(x-ct)], \quad A \ll 1. \tag{13}$$

The solution of Eq. (2) is assumed in the form

$$\psi_1 = \phi(y)\eta_1. \tag{14}$$

The position of the interface is at $Y = \alpha\eta_1$; or equivalently at $y = 1 + \eta_1$. The boundary conditions are transferred to the mean interface $y = 1$ (or $Y = 0$) by expanding them in Taylor series. Substituting Eq. (14) into Eqs. (2)–(6) and keeping only linear terms in the disturbance quantities, we obtain the following equations governing the liquid problem:

$$\phi^{iv} - 2\alpha^2\phi'' + \alpha^4\phi = i\alpha R(y-c)(\phi'' - \alpha^2\phi), \tag{15a}$$

$$\phi(0) = 0, \quad \phi'(0) = 0, \tag{15b}$$

$$c = 1 + \phi(1), \tag{15c}$$

$$\phi''' - 3\alpha^2\phi' = i\hat{\Lambda} + i\alpha R\,[\alpha^2 W - G - (c-1)\phi' - \phi]$$

$$\text{at} \quad y = 1, \tag{15d}$$

$$\phi'' + \alpha^2\phi = \hat{\chi} \quad \text{at} \quad y = 1, \tag{15e}$$

where we have assumed

$$\Lambda_1 = \hat{\Lambda}\eta_1, \quad \chi_1 = \hat{\chi}\eta_1. \tag{16}$$

Equation (15a) is the Orr–Sommerfeld equation for a linear basic-state velocity profile while, together with the boundary conditions, forms an eigenvalue problem for the complex wavespeed c. The pressure and shear perturbation coefficients $\tilde{\Lambda}$ and $\tilde{\chi}$ are determined from the analysis of the gas phase. Details of the gas problem and its solution are given by Lekoudis *et al.*[12] From the solution of the gas problem, we calculate the coefficients $\tilde{\Lambda}$ and $\tilde{\chi}$. The Orr–Sommerfeld equation is transformed into a system of four first-order equations and then solved numerically.

Figure 2 shows the variation of the wavespeed with wavenumber. It shows that one can find waves having commensurable wavenumbers and at the same time having identical (or almost identical) phase speeds. Hence, resonance conditions (interaction of harmonics) exist, and energy can be transferred between the interacting harmonics. The lowest-order interaction, and the easiest to analyze, is the second-harmonic resonant case. The experiments of Saric *et al.*[2] show, for the case of a turbulent gas, two dominant frequencies at each liquid Reynolds number. Probably the same situation occurs for the case of a laminar gas, but since the fre-

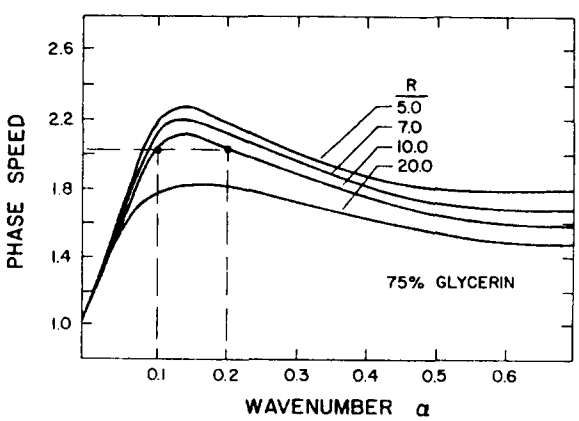

FIG. 2. The variation of the phase speed c_r with the wavenumber α.

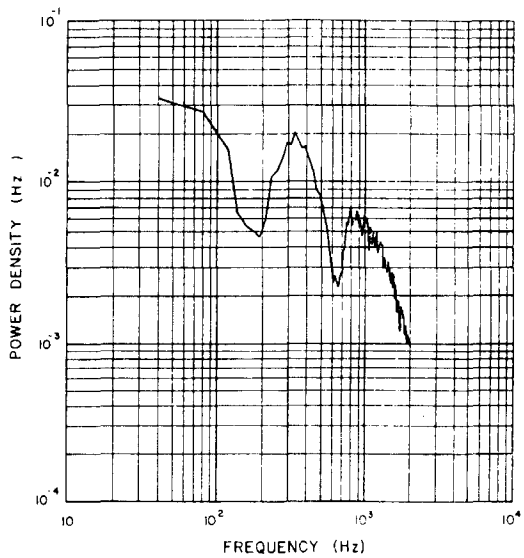

FIG. 3. Power spectral density versus frequency of the liquid surface elevation for a turbulent boundary layer. Liquid Reynolds number is 5.7.

quencies are much lower, they could not be accurately measured. Figure 3, from Saric *et al.*[2], shows that although the spectrum is continuous, the energy is concentrated around two frequencies which are in the ratio of 2 to 1. Thus, we proceed to analyze the case of the second-harmonic resonant interactions.

IV. SECOND-HARMONIC RESONANT INTERACTIONS

The present analysis uses the gas model of Lekoudis *et al.*[12] which does not restrict the extent of the disturbance layer to regions close to the wall in which the mean profiles are linear. The liquid analysis is an extension of the solution of the second-harmonic resonance of a gas over an initially quiescent liquid given by Nayfeh.[13]

We shall assume a small, but finite-amplitude disturbance of the liquid surface. Defining the parameter ϵ as the ratio of the wave amplitude to the mean depth, we let

$$\psi = \epsilon\psi_1 + \epsilon^2\psi_2 + O(\epsilon^3), \tag{17a}$$

$$h = 1 + \epsilon\eta_1 + \epsilon^2\eta_2 + O(\epsilon^3), \tag{17b}$$

$$p = \frac{1}{\alpha R}(\epsilon p_1 + \epsilon^2 p_2) + O(\epsilon^3), \tag{17c}$$

$$\Lambda = \epsilon\Lambda_1 + \epsilon^2\Lambda_2 + O(\epsilon^3), \tag{17d}$$

$$\chi = \epsilon\chi_1 + \epsilon^2\chi_2 + O(\epsilon^3), \tag{17e}$$

$$Q = q_0 + \epsilon\alpha q_1 + \epsilon^2\alpha q_2 + O(\epsilon^3), \tag{18}$$

where $\epsilon \ll 1$ and Q stands for any of the gas flow quantities u, v, ρ, T, P, and μ. The subscript 0 refers to the basic-state quantities. The boundary conditions at $y = h$, $[Y = \alpha(h-1)]$, are again transferred to $y = 1$, $(Y = 0)$, by expanding them in Taylor series and keeping terms up to $O(\epsilon^2)$. For temporal stability, we use the method of multiple scales[14] and introduce the slow time scale $t_1 = \epsilon t$ in addition to the fast scale $t_0 = t$. With this technique, one can determine the equations describing the time evolution of the amplitudes and phases of the waves. These equations can be used to determine periodic motion and their stability. On the other hand, the method of strained coordinates[13] (Stokes' method) yields only the periodic motions and one has to use a variational approach to study their stability.

Substituting Eqs. (17) and (18) into Eqs. (2)–(6) and Eqs. (9)–(11), expanding for small ϵ and collecting the coefficients of ϵ and ϵ^2, we obtain two sets of equations and boundary conditions governing the first-order (linear) quantities (denoted by the subscript 1) and the second-order (nonlinear) quantities (denoted by the subscript 2).

A. First-order problem

The results of Sec. III show that for the wavenumbers of interest and for any pair of wavenumbers with a two to one ratio, the complex wavespeeds c_1 and c_2, of the two harmonics, have the following properties:

$$\mathrm{Re}(c_1 - c_2) = O(\epsilon), \quad \mathrm{Im}(c_1) = O(\epsilon), \quad \mathrm{Im}(c_2) = O(\epsilon).$$

Thus, a near second-harmonic resonant condition exists. To determine a uniform expansion, we use the method of multiple scales[14] and include both the fundamental and its first harmonic in the solution of the first-order problem; i.e., we let

$$\eta_1 = \sum_{m=1}^{2} A_m(t_1)\exp(i\theta_m) + \text{c.c.}, \tag{19}$$

$$\psi_1 = \sum_{m=1}^{2} A_m(t_1)\phi_{1m}(y)\exp(i\theta_m) + \text{c.c.}, \tag{20}$$

where

$$\theta_m = m(x - c_m t_0). \tag{21}$$

The θ_m are fast varying phases and the A_m are slowly varying amplitudes.

Substituting Eqs. (19) and (20) into the first-order liquid problem, we obtain

$$\frac{dw_{1i}^{(m)}}{dy} - \sum_{j=1}^{4} \beta_{ij}^{(m)} w_{1j}^{(m)} = 0 \quad \text{for} \quad i = 1,\ldots,4, \tag{22a}$$

$$w_{11}^{(m)} = w_{12}^{(m)} = 0 \quad \text{at} \quad y = 0, \tag{22b}$$

$$w_{13}^{(m)} + \gamma_{11}^{(m)} w_{11}^{(m)} + \gamma_{12}^{(m)} w_{12}^{(m)} = im\Lambda_1^{(m)} + im\alpha R(m^2\alpha^2 W - G)$$

$$\text{at} \quad y = 1, \tag{22c}$$

$$w_{13}^{(m)} + \gamma_{21}^{(m)} w_{11}^{(m)} = \chi_1^{(m)} \quad \text{at} \quad y = 1, \tag{22d}$$

$$c_m = 1 + w_{11}^{(m)} \quad \text{at} \quad y = 1, \tag{22e}$$

where the β_{ij} and γ_{ij} are given in Appendix A, Λ_1 and χ_1 are determined from the gas analysis and defined in Appendix C, and

$$w_{n_1}^{(m)} = \phi_{nm}, \quad w_{n_2}^{(m)} = \phi'_{nm}, \quad w_{n_3}^{(m)} = \phi''_{nm}, \quad w_{n_4}^{(m)} = \phi'''_{nm}. \tag{23}$$

Similarly, the solution of the first-order gas problem is written in the form

$$f_1(x,y,t) = \sum_{m=1}^{2} A_m(t_1) f_1^{(m)}(y)\exp(i\theta_m), \tag{24}$$

where the vector f_n has the components

$$f_n = \left(u_n, \frac{\partial u_n}{\partial y}, v_n, p_n, T_n, \frac{\partial T_n}{\partial y}\right). \tag{25}$$

Substituting Eqs. (24) into the first-order problem, we obtain

$$\frac{df_{1i}^{(m)}}{dy} - \sum_{j=1}^{6} \alpha_{ij}^{(m)} f_{1i}^{(m)} = 0 \quad \text{for} \quad i = 1,\ldots,6, \tag{26a}$$

$$f_{11}^{(m)} = -u_0', \quad f_{13}^{(m)} = 0, \quad f_{15}^{(m)} = -T_0', \tag{26b}$$

where the α_{ij} are defined in Appendix B.

B. Second-order problem

Substituting the first-order (linear) solution into the second-order (nonlinear) problem leads to an inhomogeneous set of equations and boundary conditions. Since the homogeneous part of these equations is the same as the first-order problem, the first-order problem has a solution if, and only if, a solvability condition is satisfied (i.e., secular terms are eliminated). We note that since the fundamental and its harmonic travel with approximately the same phase speed, all terms proportional to $\exp[i(\theta_2 - \theta_1)]$ and $\exp(2\theta_1)$ as well as those proportional to $\exp(i\theta_1)$ and $\exp(i\theta_2)$ produce secular terms.

To determine the solvability conditions, we seek a particular solution for the second-order problem in the form

$$\eta_2 = \sum_{m=1}^{2} B_m \exp(i\theta_m) + \text{c.c.}\,, \tag{27}$$

$$\psi_2 = \sum_{m=1}^{2} B_m(y)\phi_{2m} \exp(i\theta_m) + \text{c.c.} \tag{28}$$

Substituting Eqs. (27) and (28) into the second-order equations and equating the coefficients of $\exp(i\theta_m)$ on both sides, we obtain

$$\frac{dw_{2i}^{(m)}}{dy} - \sum_{j=1}^{4} \beta_{ij}^{(m)} w_{2j}^{(m)} = M_i^{(m)}\,, \quad i = 1,...,4\,, \tag{29a}$$

$$w_{21}^{(m)} = w_{22}^{(m)} = 0 \quad \text{at} \quad y = 0\,, \tag{29b}$$

$$w_{24}^{(m)} + \gamma_{11}^{(m)} w_{21}^{(m)} + \gamma_{12}^{(m)} w_{22}^{(m)} = im\Lambda_3^{(m)} + im\alpha R\,[(m\alpha)^2 W - G\,]B_m + M_5^{(m)}\,, \tag{29c}$$

$$w_{23}^{(m)} + \gamma_{21}^{(m)} w_{21}^{(m)} = \chi_2^{(m)} + M_6^{(m)} \quad \text{at} \quad y = 1\,, \tag{29d}$$

$$w_{21}^{(m)} = (c_m - 1)B_m + M_7^{(m)} \quad \text{at} \quad y = 1\,, \tag{29e}$$

where the w_{nm} are defined in Eq. (23) and the M_i are inhomogeneities which are functions of the first-order problem and defined in Appendix A along with the β_{ij} and γ_{ij}.

Similarly, we seek a particular solution for the second-order gas problem in the form

$$f_2 = \sum_{m=1}^{2} f_2^{(m)}(Y)\exp(i\theta_m)\,, \tag{30}$$

where the vector f_n is defined in Eq. (25). Substituting Eqs. (29) into the second-order gas problem, we obtain

$$\frac{df_{2i}^{(m)}}{dY} - \sum_{i=1}^{6} \alpha_{ij}^{(m)} f_{2j}^{(m)} = N_i^{(m)}\,, \tag{31}$$

where the α_{ij} are defined in Appendix B and the $N_i^{(m)}$ are functions of the first-order gas problem and defined in Appendix C. It follows from Eqs. (11) that the wall boundary conditions can be rewritten as

$$f_{21}^{(m)} = -B_m u_0' + N_7^{(m)} \quad \text{at} \quad Y = 0\,, \tag{32a}$$

$$f_{23}^{(m)} = -N_8^{(m)} \quad \text{at} \quad Y = 0\,, \tag{32b}$$

$$f_{25}^{(m)} = -B_m T_0' + N_9^{(m)} \quad \text{at} \quad Y = 0\,. \tag{32c}$$

Moreover, it follows from Eqs. (5) and (6) that the second-order pressure and shear perturbation parameters Λ and χ can be rewritten as

$$im\Lambda_2^{(m)} = \frac{-2(m\alpha)^2\mu_0(0)}{R_G} f_{21}^{(m)} + \frac{im\alpha^2}{c_f} f_{24}^{(m)} + N_{10}^{(m)} = \delta_1^{(m)} f_{21}^{(m)} + \delta_4^{(m)} f_{24}^{(m)} + N_{10}^{(m)}\,, \tag{33}$$

$$\chi_2^{(m)} = \frac{\alpha\mu_0(0)}{c_f R_G} f_{22}^{(m)} + \frac{\alpha b_1 u_0'(0)\mu_0(0)}{c_f R_G} f_{25}^{(m)} + N_{11}^{(m)} = r_2^{(m)} f_{22}^{(m)} + r_5^{(m)} f_{25}^{(m)} + N_{11}^{(m)}\,. \tag{34}$$

C. Solvability condition

To determine the solvability condition of the second-order problem, we multiply Eq. (29a) by the functions $W_i^{(m)}$, $i = 1,2,...,4$, Eq. (31) by the functions $F_i^{(m)}$, $i = 1,2,...,6$, where the W_i and F_m are defined below, add the results, and then integrate by parts in the corresponding intervals to transfer the derivatives from w_i and f_i to W_i and F_i. The result is

$$\sum_{i=1}^{4} w_{2i}^{(m)} W_i^{(m)}\Big|_0^1 - \int_0^1 \left(\frac{dW_i^{(m)}}{dy} + \sum_{j=1}^{4} \beta_{ji}^{(m)} W_j^{(m)}\right) w_{2i}^{(m)}\, dy + \sum_{i=1}^{6} f_{2i}^{(m)} F_i^{(m)}\Big|_0^\infty - \int_0^\infty \left(\frac{dF_i^{(m)}}{dY} + \sum_{j=1}^{6} \alpha_{ji}^{(m)} F_j^{(m)}\right) f_{2i}^{(m)}\, dY = \sum_{i=1}^{4} \int_0^1 M_i W_i\, dy + \sum_{i=1}^{6} \int_0^\infty N_i F_i\, dy\,. \tag{35}$$

We choose the $W_i^{(m)}$ and the $F_i^{(m)}$ to be solutions of the adjoint homogeneous problem:

$$\frac{dW_i^{(m)}}{dy} + \sum_{j=1}^{4} \beta_{ji}^{(m)} W_j^{(m)} = 0\,, \quad i = 1,2,...,4\,, \tag{36}$$

$$\frac{dF_i^{(m)}}{dY} + \sum_{j=1}^{6} \alpha_{ji}^{(m)} F_j^{(m)} = 0\,, \quad i = 1,2,...,6\,, \tag{37}$$

$$W_3^{(m)} = W_4^{(m)} = 0 \quad \text{at} \quad y = 0\,, \tag{38a}$$

$$W_2^{(m)} - \gamma_{12}^{(m)} W_4^{(m)} = 0 \quad \text{at} \quad y = 1\,, \tag{38b}$$

$$(c_m - 1)W_1^{(m)} + [\gamma_{21}^{(m)}(1 - c_m) - r_5^{(m)} T_0'\,] W_3^{(m)} + [im\alpha R\,(m^2\alpha^2 W - G\,) - \delta^{(m)} u_0' + \gamma_{11}^{(m)}(1 - c_m)\,] W_4^{(m)} + u_0' F_1^{(m)} + T_0' F_5^{(m)} = 0 \quad \text{at} \quad y = 1 \quad \text{and} \quad Y = 0 \tag{38c}$$

$$F_2^{(m)} - r_2^{(m)} W_3^{(m)} = 0 \quad \text{at} \quad y = 1 \quad \text{and} \quad Y = 0\,, \tag{38d}$$

$$F_4^{(m)} - \delta_4^{(m)} W_4^{(m)} = 0 \quad \text{at} \quad y = 1 \quad \text{and} \quad Y = 0\,, \tag{38e}$$

$$F_6^{(m)} = 0 \quad \text{at} \quad Y = 0\,, \tag{38f}$$

$$F_i^{(m)} < \infty \quad \text{as} \quad Y \to \infty\,. \tag{38g}$$

With this choice for the $W_i^{(m)}$ and $F_i^{(m)}$, Eq. (35) yields the following solvability condition:

$$\sum_{i=1}^{4} \int_0^1 M_i^{(m)} W_i^{(m)} dy + \sum_{i=1}^{6} \int_0^\infty N_i^{(m)} F_i^{(m)} dY + [(\delta_1^{(m)} W_4^{(m)} - W_1^{(m)}) N_7^{(m)} - N_8^{(m)} F_3^{(m)} + (r_5^{(m)} W_3^{(m)} - F_3^{(m)}) N_9^{(m)} + (W_2^{(m)} - \gamma_{21}^{(m)} W_3^{(m)} - \gamma_{11}^{(m)} W_4^{(m)}) M_7^{(m)} + W_4^{(m)}(M_5^{(m)} + N_{10}^{(m)}) + W_3^{(m)}(M_6^{(m)} + N_{11}^{(m)})]_{y=1,Y=0} = 0\,. \tag{39}$$

Substituting for the M_i and N_i from Appendices A and C into Eq. (39), substituting for η_1, ψ_1, and $f_{1i}^{(m)}$ from Eqs. (19), (20), and (24) into the resulting equation, and rearranging, we obtain

$$\frac{dA_1}{dt_1} + E_1 \bar{A}_1 A_2 \exp[i\,\mathrm{Re}(\theta_2 - 2\theta_1) + 2\,\mathrm{Im}(c_2)t_0] = 0\,, \tag{40}$$

$$\frac{dA_2}{dt_1} + E_2 A_1^2 \exp[-i\,\mathrm{Re}(\theta_2 - 2\theta_1) + 2\,\mathrm{Im}(c_1 - c_2)t_0] = 0 \tag{41}$$

where E_1 and E_2 are defined in Appendix A and Re and Im denote the real and imaginary parts, respectively. Letting

$$A_m^* = A_m(t_1)\exp[m\,\mathrm{Im}(c_m)t_0]\,, \tag{42}$$

$$\Gamma = 2\epsilon^{-1}\,\mathrm{Re}(c_1 - c_2)\,, \tag{43}$$

$$E_m = 2\zeta_m \exp(i\tau_m), \quad A^*_m = \tfrac{1}{2}a_m \exp(i\beta_m), \tag{44}$$

and separating real and imaginary parts in Eqs. (40) and (41), we obtain

$$\frac{da_1}{dt_1} - \mathrm{Im}(c_1)a_1 + \zeta_1 a_1 a_2 \cos(\beta_2 - 2\beta_1 + \tau_1 + \Gamma t_1) = 0, \tag{45}$$

$$\frac{d\beta_1}{dt_1} + \zeta_1 a_2 \sin(\beta_2 - 2\beta_1 + \tau_1 + \Gamma t_1) = 0, \tag{46}$$

$$\frac{da_2}{dt_1} - 2\,\mathrm{Im}(c_2)a_2 + \zeta_2 a_1^2 \cos(-\beta_2 + 2\beta_1 + \tau_2 - \Gamma t_1) = 0, \tag{47}$$

$$a_2 \frac{d\beta_2}{dt_1} + \zeta_2 a_1^2 \sin(-\beta_2 + 2\beta_1 + \tau_2 - \Gamma t_1) = 0. \tag{48}$$

These equations govern the time modulation of the amplitudes and the phases of the interacting harmonics.

We note that because of the form of the interface boundary conditions, the *adjoint* problem is *coupled* to the liquid motion, in contrast with the *eigensolution* in which the gas problem is *decoupled* from the liquid problem. A discussion of this is given in Ref. 14. The solution of the adjoint problem also provides a check on the eigenvalues determined from the solution of the first-order problem. It should be mentioned that the discontinuity between the curves shown in Figs. 5–7 is due to the change in the water/glycerin mixture that alters the liquid surface velocity and depth. Thus the nondimensionalizing parameters change. Details about the liquid flow conditions can be found in Ref. 2.

The numerical solutions of the first-order gas problem given by Eq. (26) and the adjoint problem given by Eqs. (37)–(38) encountered computational difficulties characteristic of solutions of the Orr–Sommerfeld equation when the Reynolds number is large. Therefore, these calculations were carried out using a special computer code[15] utilizing superposition and a modified Gram–Schmidt orthonormalization procedure in order to minimize parasitic error growth in the solutions.

V. RESULTS AND DISCUSSIONS

The solutions of the first-order problem and its adjoint provide the coefficients ζ_1, ζ_2, τ_1, and τ_2 of Eqs. (45)–(48). This system and the initial values for the wave amplitudes constitute an initial value problem for a_1 and a_2. Since these initial conditions are unknown and since we are examining self-sustained oscillations and the experiments indicate stable finite-amplitude waves, it is of interest to look at the steady-state solutions of Eqs. (45)–(48).

For the case of phase-modulated waves, the steady-state amplitudes are given by

$$\mathrm{Im}(c_1) - \zeta_1 a_2 \cos(\beta_2 - 2\beta_1 + \Gamma t_1 + \tau_1) = 0 \tag{49a}$$

$$2\,\mathrm{Im}(c_2)a_2 - \zeta_2 a_1^2 \cos(-\beta_2 + 2\beta_1 - \Gamma t_1 + \tau_2) = 0 \tag{49b}$$

$$\Gamma a_2 + \zeta_2 a_1^2 \sin(-\beta_2 + 2\beta_1 - \Gamma t_1 + \tau_2) + 2\zeta_1 a_1^2 \sin(\beta_2 - 2\beta_1 + \Gamma t_1 + \tau_1) = 0 \tag{49c}$$

$$\beta_2 - 2\beta_1 + \Gamma t_1 = \text{const}. \tag{49d}$$

Equations (49) have been solved by using a standard Newton–Raphson iteration scheme. In the case of a laminar boundary layer one needs computing times the order of 60 minutes on an IBM 370/158 computer to span the range of wavenumbers from 0 to 0.5 in steps of 0.05. In the case of a turbulent gas boundary layer, the computation time increases to 10 hours because of hundreds of needed orthonormalizations across the boundary layer. In this case, we assume that the disturbance field is uncorrelated with the turbulent fluctuations[12] to $O(\epsilon^2)$.

Figure 4 shows the variation of the steady-state amplitudes with wavenumber for a liquid Reynolds of 3.0. The predicted wave amplitudes are the order of the observed ones. This constitutes an improvement over the previous nonlinear results which overpredict the maximum amplitudes by an order of magnitude.[10] For the case of high wavenumbers, the second harmonic is highly attenuated and the iteration scheme fails to converge.

Figure 5 compares the predicted and observed r.m.s. wave amplitudes. The agreement is good for the 40/60 water/glycerin mixture. Moreover, the results show that the

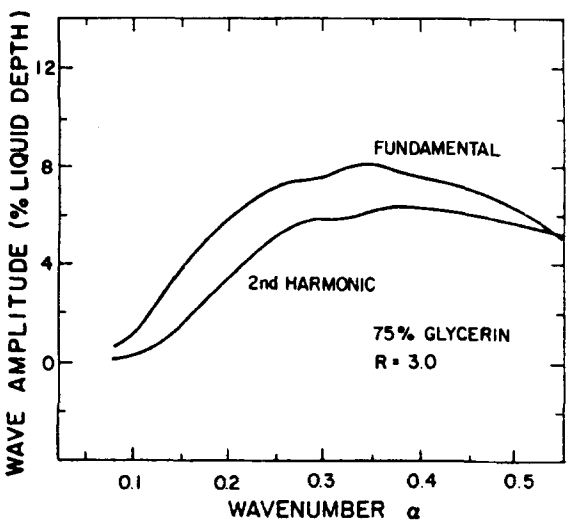

FIG. 4. Predicted variation of the harmonic amplitudes with wavenumbers.

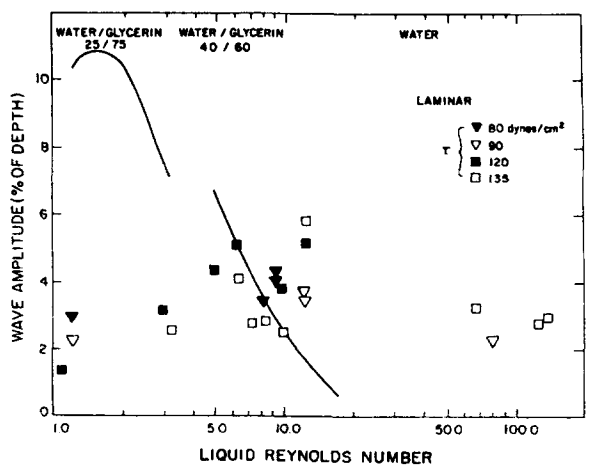

FIG. 5. Comparison of predicted and observed r.m.s. wave amplitudes.

wave amplitude decreases as the liquid Reynolds number increases. This implies that the effect of the second-harmonic resonance is less important at the higher liquid Reynolds numbers. The present model is an improvement over the models of Refs. 1, 2, and 10. However, the solution is still useful only in the intermediate range of Reynolds numbers as was the model of Ref. 10. This limitation is due to the fact that the wave speed approaches unity as the liquid Reynolds number becomes large and therefore, more than two waves can strongly interact.[1,11] At large Reynolds numbers, the calculated amplitudes are unrealistic because they are bigger than the mean liquid depth. Consequently, the present model is inadequate for large liquid Reynolds numbers.

For the case of low Reynolds number, the results overpredict the amplitudes by a factor of about 3. It should be mentioned that the experiments with a turbulent boundary layer do not show a second frequency for this range of Reynolds numbers.

The experiments show that, although there is a dominant frequency at each Reynolds number, and in some cases, a dominant fundamental and second harmonic, the spectrum contains also the higher harmonics. Moreover, the results of the linear solution indicate the possibility of the interaction of the fundamental frequency with its second and third harmonics, as can be seen in Fig. 2. Therefore, the range of validity of the present model could be extended by adding more harmonics to the solution. However, the algebraic labor would increase considerably because of complexities in the gas problem.

Figures 6 and 7 compare the predicted and observed frequencies and wavenumbers. These results show that the present model constitutes an improvement over the previous models.[2,10] Additional solutions of the system were not found despite a numerical search with different initial guesses. The steady-state amplitudes calculated using this model suggest that, for the intermediate range of liquid-Reynolds numbers, the observed waves are a result of this type of interaction. For the higher liquid-Reynolds numbers more harmonics are probably needed to predict the amplitudes.

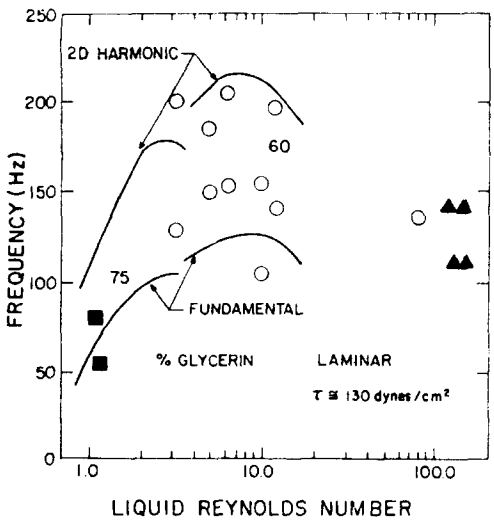

FIG. 6. Comparison of predicted and observed frequencies. (The different symbols denote different glycerin/water mixtures: ■ 75%, ○ 60%, ▲ 0%.)

The present nonlinear analysis is capable of predicting part of the experimental observations. Including the third harmonic in the analysis may extend the validity of the analysis to higher liquid-Reynolds numbers. However, the algebraic labor and the computational time involved would increase considerably. Also, three-dimensional effects need to be considered. A simple analysis with a linear model would determine if conditions for strong nonlinear wave-wave interactions are present. Furthermore, the effects of mass transfer at the interface need to be ascertained. Although the mass transfer slightly affects the eigenvalues[6] for the problem of slag deposition in an MDH generator, it may have a non-negligible effect on the nonlinear problem through changes in the eigenfunctions.

ACKNOWLEDGMENTS

The authors would like to acknowledge the help of M. R. Scott and H. A. Watts of Sandia Laboratories in using their computer code, SUPORT.[15]

This work was supported by the Fluid Dynamics Program of the Office of Naval Research.

APPENDIX A

$$\beta_{11}^{(m)} = \beta_{13}^{(m)} = \beta_{14}^{(m)} = 0\,, \quad \beta_{12}^{(m)} = 1\,, \tag{A1}$$

$$\beta_{21}^{(m)} = \beta_{22}^{(m)} = \beta_{24}^{(m)} = 0\,, \quad \beta_{23}^{(m)} = 1\,, \tag{A2}$$

$$\beta_{31}^{(m)} = \beta_{32}^{(m)} = \beta_{33}^{(m)} = 0\,, \quad \beta_{34}^{(m)} = 1\,, \tag{A3}$$

$$\beta_{41}^{(m)} = -(m\alpha)^3[m\alpha + iR(y - c_m)]\,, \quad \beta_{42}^{(m)} = 0\,, \tag{A4}$$

$$\beta_{43}^{(m)} = (m\alpha)[2m\alpha + iR(y - c_m)]\,, \quad \beta_{44}^{(m)} = 0\,, \tag{A5}$$

$$\gamma_{11}^{(m)} = im\alpha R\,, \quad \gamma_{12}^{(m)} = -3(m\alpha)^2 + im\alpha R(c_m - 1)\,, \tag{A6}$$

$$\gamma_{21}^{(m)} = (m\alpha)^2\,, \tag{A7}$$

$$M_1^{(m)} = M_2^{(m)} = M_3^{(m)} = 0\,, \tag{A8}$$

$$M_4^{(m)} = \alpha R(\psi_{1y}\psi_{1xyy} - \psi_{1x}\psi_{1yyy}) + \alpha^3 R(\psi_{1y}\psi_{1xxx} - \psi_{1x}\psi_{1xxy})\,, \tag{A9}$$

$$M_5^{(m)} = \frac{\partial}{\partial x}\left[-2\alpha^2(\psi_{1yy} - \alpha^2\psi_{1xx})\eta_{1x} - (p_{1y} + 2\alpha^2\psi_{1xyy})\eta_1\right] \quad \text{at} \quad y = 1\,, \tag{A10}$$

$$M_6^{(m)} = 4\alpha^2\psi_{1xy}\eta_{1x} - \eta_1(\psi_{1yyy} - \alpha^2\psi_{1xxy}) \quad \text{at} \quad y = 1\,, \tag{A11}$$

$$M_7^{(m)} = -(\eta_1 + \psi_{1y})\eta_1 - \eta_1\psi_{1xy} \quad \text{at} \quad y = 1\,, \tag{A12}$$

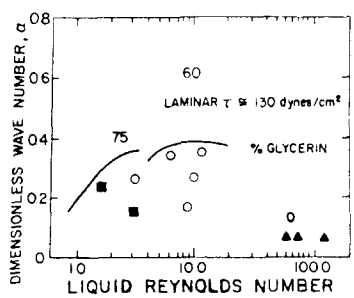

FIG. 7. Comparison of predicted and observed wavenumbers. (The different symbols denote different glycerin/water mixtures: ■ 75%, ○ 60%, ▲ 0%.)

APPENDIX B

$$\alpha_{11}^{(m)}=\alpha_{13}^{(m)}=\alpha_{14}^{(m)}=\alpha_{15}^{(m)}=\alpha_{16}^{(m)}=0\,,\quad \alpha_{12}^{(m)}=1\,, \tag{B1}$$

$$\alpha_{21}^{(m)}=m^2+imR_G\,,\quad \alpha_{22}^{(m)}=\alpha_{23}^{(m)}=0\,,$$

$$\alpha_{24}^{(m)}=-(m^2/3)\gamma M_\infty^2+imR_G\,,$$

$$\alpha_{25}^{(m)}=m^2/3\,,\quad \alpha_{26}^{(m)}=0\,, \tag{B2}$$

$$\alpha_{31}^{(m)}=-im\,,\quad \alpha_{32}^{(m)}=\alpha_{33}^{(m)}=0\,,\quad \alpha_{34}^{(m)}=-im\gamma M_\infty^2\,,$$

$$\alpha_{35}^{(m)}=im\,,\quad \alpha_{36}^{(m)}=0\,, \tag{B3}$$

$$\alpha_{41}^{(m)}=0\,,\quad \alpha_{42}^{(m)}=-im/\left[R_G+(4i/3)m\gamma M_\infty^2\right],$$

$$\alpha_{43}=(-m^2-imR_G)/\left[R_G+(4i/3)\,m\gamma M_\infty^2\right],$$

$$\alpha_{44}^{(m)}=\alpha_{45}^{(m)}=0\,,\quad \alpha_{46}^{(m)}=\tfrac{4}{3}im/(R_G+\tfrac{4}{3}im\gamma M_\infty^2)\,, \tag{B4}$$

$$\alpha_{51}^{(m)}=\alpha_{52}^{(m)}=\alpha_{53}^{(m)}=\alpha_{54}^{(m)}=\alpha_{55}^{(m)}=0\,,\quad \alpha_{56}^{(m)}=1\,, \tag{B5}$$

$$\alpha_{61}^{(m)}=\alpha_{62}^{(m)}=\alpha_{63}^{(m)}=0\,,\quad \alpha_{64}^{(m)}=-imRPr(\gamma-1)M_\infty^2\,,$$

$$\alpha_{65}^{(m)}=imR_GPr+m^2\,,\quad \alpha_{66}^{(m)}=0\,. \tag{B6}$$

APPENDIX C

$$im\Lambda_1^{(m)}=-\frac{2(m\alpha)^2\mu_0(0)}{R_G}f_{21}^{(m)}+\frac{im\alpha^2}{c_f}f_{24}^{(m)}, \tag{C1}$$

$$\chi_1^{(m)}=\frac{\alpha\mu_0(0)}{c_fR_G}f_{22}^{(m)}+\frac{\alpha b_1U_0'(0)\mu_0(0)}{c_fR_g}f_{25}^{(m)}, \tag{C2}$$

where $b_1=\mu_0\left[\tfrac{3}{2}T_0^{-1}-(T_0+b)^{-1}\right]$.

$$N_1^{(m)}=N_5^{(m)}=0\,, \tag{C3}$$

$$\begin{aligned}N_2^{(m)}=&-\frac{b_2'u_0'}{\mu_0}T_1^2-\frac{2b_2u_0'}{\mu_0}T_1T_1'-\frac{im}{3}N_3^{(m)}\\&+(\alpha R_G/\mu_0)\{(\rho_1u_0+\rho_0u_1)u_{1x}+(\rho_1u_0'+\rho_0u_{1Y})v_1\\&-(1/\mu_0)\left[\mu_1(u_{1YY}+\tfrac{4}{3}\mu_{1xx}+\tfrac{1}{3}v_{1xY})\right.\\&\left.+\mu_{1x}(\tfrac{4}{3}u_{1x}-\tfrac{2}{3}v_{1Y})+\mu_{1Y}(u_{1Y}+v_{1x})\right]\}\,,\end{aligned} \tag{C4}$$

$$\begin{aligned}N_3^{(m)}=&-\alpha\left[\rho_{1x}u_1+\rho_1u_{1x}+\rho_{1Y}v_1\right.\\&\left.+v_{1Y}\rho_1+(u_0/T_0)(\rho_1T_1)_x\right]\,,\end{aligned} \tag{C5}$$

$$\begin{aligned}N_4^{(m)}=&\left\{\frac{4\mu_0}{3}\left(\frac{T_0'}{T_0}N_3^{(m)}+\frac{dN_3^{(m)}}{dY}+\frac{4\mu_0'}{3}N_3^{(m)}\right)+2b_1u_0'T_1T_{1x}\right.\\&-\alpha R\left[(\rho_0u_1+\rho_1u_0)v_{1x}+\rho_0v_1v_{1Y}\right]\\&+\alpha\left[\mu_1\left(v_{1xx}+\frac{4}{3}v_{1YY}+\frac{1}{3}u_{1xY}\right)\right.\\&\left.\left.+\mu_{1x}(\mu_{1Y}+v_{1x})+\mu_{1Y}\left(\frac{4}{3}v_{1YY}+\frac{2}{3}u_{1x}\right)\right]\right\}\\&\times(R_G+\tfrac{4}{3}im\mu_0M_\infty u_0)^{-1}\,,\end{aligned} \tag{C6}$$

$$\begin{aligned}N_6^{(m)}=&-\frac{(\gamma-1)M_\infty^2b_1\,\mathrm{Pr}}{\mu_0}T_1^2-\frac{2b_1T_0'}{\mu_0}T_1T_{1Y}-\frac{T_0'b_2'}{\mu_0}T_1^2\\&-\frac{b_1T_0''}{\mu_0}T_1^2+(R_G\,\mathrm{Pr}\,\alpha/\mu_0)(\rho_0u_1+\rho_1u_0)T_{1x}\\&+((\rho_0T_{1Y}+\rho_1T_0')v_1-(\gamma-1)M_\infty^2\\&\times\{u_1p_{1x}+v_1p_{1Y}+(1/R_G)\left[2\mu_1u_0'(\mu_{1Y}+v_{1x})\right.\\&+\tfrac{4}{3}(u_{1x}^2+v_{1y}^2)-\tfrac{4}{3}(u_{1x}+v_{1y}^2)\\&\left.-\tfrac{4}{3}u_{1x}v_{1y}+(u_{1Y}+v_{1x})^2\right]\}\\&+(1/R_G\mathrm{Pr})(\mu_{1x}T_{1x}+\mu_1T_{1xx}+\mu_{1Y}T_{1Y}+\mu_1T_{1YY}))\end{aligned} \tag{C7}$$

$$N_7^{(m)}=-\alpha(u_{1Y}\eta_1+\tfrac{1}{2}u_0''\eta_1^2)\quad\text{at}\quad Y=0\,, \tag{C8}$$

$$N_8^{(m)}=-\alpha v_{1Y}\eta_1\quad\text{at}\quad Y=0\,, \tag{C9}$$

$$N_9^{(m)}=-\alpha(T_{1Y}\eta_1+\tfrac{1}{2}T_0''\eta_1^2)\,,\quad\text{at}\quad Y=0\,, \tag{C10}$$

$$\begin{aligned}N_{10}^{(m)}=&-\frac{4\mu_0}{3R_G}N_3^{(m)}+\alpha\left(p_{1Y}+\frac{2\mu_0}{R_G}(u_{1xY}-2v_{1YY})\right)\\&+\alpha\frac{2\mu_1}{3R_G}(\mu_{1x}+v_{1Y})-\frac{2\mu_1}{R_G}v_{1Y}\\&+\frac{2\mu_0\eta_{1x}}{R_G}(\mu_{1Y}+v_{1x})+\frac{2}{R_G}\mu_1(\mu_0'\eta_{1x})\quad\text{at } Y=0\end{aligned} \tag{C11}$$

$$\begin{aligned}N_{11}^{(m)}=&\frac{im\mu_0\alpha}{R_G}v_{1Y}+\eta_1\frac{b_1u_0'}{R_G}T_1^2+\frac{\alpha\eta_1}{R_G}\\&\times\left[\mu_0u_{1YY}+\mu_0'(v_{1xY}+u_{1Y})+\mu_1u_0''+\mu_{1Y}u_0'\right]\\&+\frac{\alpha}{R_G}\left[\mu_1u_{1Y}+2\mu_0\eta_{1x}(v_{1Y}-u_{1x})\right]\quad\text{at}\quad Y=0\,,\end{aligned} \tag{C12}$$

where

$$b_2=\mu_0\left[\tfrac{1}{8}T_0^{-2}+(T_0+b)^{-2}-\tfrac{3}{2}T_0^{-1}(T_0+b)^{-1}\right].$$

APPENDIX D

$$\begin{aligned}E_{(m)}=&\left(-\sum_{i=1}^{6}\int_0^\infty N_i^{(m)}F_i^{(m)}\,dY-\sum_{i=1}^{4}\int_0^1M_i^{(m)}W_i^{(m)}\,dy\right.\\&+\left[(\delta_1^{(m)}W_4^{(m)}-F_1^{(m)})N_7^{(m)}-N_8^{(m)}F_3^{(m)}\right.\\&+(r_5^{(m)}W_3^{(m)}-F_5^{(m)})N_9^{(m)}+(W_1^{(m)}\\&-\gamma_{21}^{(m)}W_3^{(m)}-\gamma_{11}^{(m)}W_4^{(m)})M_7^{(m)}+(N_5^{(m)}+M_{10}^{(m)})W_4^{(m)}\\&\left.\left.+(M_5^{(m)}+N_{11}^{(m)})W_3^{(m)}\right]_{\substack{Y=0\\y=1}}\right)\\&\times\left(\alpha R\int_0^1\left[\phi_m''-(m\alpha)^2\phi_m\right]W_4^{(m)}dy\right.\\&\left.+(W_1^{(m)}-\gamma_{21}^{(m)}W_3^{(m)}-\gamma_{11}^{(m)}W_4^{(m)})_{\substack{Y=0\\y=1}}\right)^{-1}.\end{aligned} \tag{D1}$$

[1] G. L. Bordner, A. H. Nayfeh, and W. S. Saric, ZAMP **26**, 771 (1975).
[2] W. S. Saric, A. H. Nayfeh, and S. G. Lekoudis, J. Fluid Mech. **77**, 63 (1976).
[3] D. E. Wurz, Dr. Ing. thesis, Universität Karlsruhe, 1971.
[4] S. Kim, Dr. Ing. thesis, Universität Karlsruhe, 1976.
[5] D. E. Wurz, Arch. Mech. Stosow. **26**, 969 (1976).
[6] W. S. Saric, K. J. Touryan, and M. R. Scott, J. Energy **1**, 108 (1977).
[7] R. L. Gater and M. R. L'Ecuyer, Int'l J. Heat Mass Trans. **13**, 1925 (1971).
[8] A. H. Nayfeh and W. S. Saric, J. Fluid Mech. **46**, 209 (1971).
[9] A. H. Nayfeh and W. S. Saric, J. Fluid Mech. **58**, 39 (1973).
[10] G. L. Bordner and A. H. Nayfeh, Virginia Polytechnic Institute and State University, Technical Report No. VPI-E-74-11 (1974).
[11] S. G. Lekoudis, Ph. D. dissertation, Virginia Polytechnic Institute and State University, 1977.
[12] S. G. Lekoudis, A. H. Nayfeh, and W. S. Saric, Phys. Fluids **19**, 514 (1976).
[13] A. H. Nayfeh, J. Fluid Mech. **59**, 803 (1973).
[14] A. H. Nayfeh, *Perturbation Methods* (Wiley, New York, 1973), Chap. 6.
[15] M. R. Scott and H. A. Watts, SIAM J. Num. Anal. **14**, 40 (1977).